

NARROW BAND RED EMISSION IN EUROPIUM ACTIVATED CERIA NANOCRYSTALS

B. S. CHAKRABARTY

Department of Applied Physics, Faculty of Technology & Engineering, M.S. University of Baroda,
Vadodara, Gujarat, India

ABSTRACT

Europium activated Ceria nanocrystals having 14.8 nm crystallite size, prepared by precipitation method exhibit very narrow emission band at 590 nm with high intensity. This is significant as the width of the peak is not more than a few nano meters and the intensity is quite high. The material is likely to have a high efficiency of conversion.

KEYWORDS: Cerium Oxide, Narrow Emission, Ceria Nano Meters

INTRODUCTION

Systems involving rare earth oxides, especially Cerium, have many practical applications due to their excellent physical and chemical properties^[1]. Cerium oxide (CeO_2) powders have attracted much attention owing to their potential uses in a variety of applications, e.g. UV absorbents and filters^[2, 3], as catalysts for the treatment of automotive exhaust system because of its high oxygen ion conductivity^[4] and petroleum-cracking catalyst^[5]. Rare-earth-doped Ceria have been considered promising materials as oxygen ion conducting electrolytes or electrodes for Solid Oxide Fuel Cell (SOFC)^[6], oxygen pumps^[7, 8] and oxygen sensors^[9]. It is also used as polishing agents for the chemical mechanical planarization (CMP) process, gate oxides in metal oxide semiconductor devices and ultraviolet (UV) blocking materials in UV shielding^[10, 11]. Ceria nano particles are being used in many biomedical applications due to their nontoxic nature and excellent biocompatibility^[12].

Europium belongs to the rare earth metal group and has a strong red emission when doped in different matrices.^[13, 14, 15] Europium is considered as a suitable dopant for enhancing emission in Ceria for three reasons: (i) it can be excited in a wide range of wavelengths from ultraviolet to visible light,^[16] (ii) the ionic radius of Eu^{3+} (0.1066 nm), being close to that of Cerium (Ce^{3+} , 0.1143 nm; Ce^{4+} , 0.097 nm), favours extensive solubility with the Ceria lattice, and (iii) it increases the trivalent state of Cerium, which may further enhance the applicability of Ceria. Therefore Europium doped Ceria can be used in fluorescence applications.

Cerium provides strong absorption below 400 nm caused by charge transfer bands^[17]. Due to its high refractive index, optical transparency, thermal and chemical stability, high dielectric constant (26) and its good compatibility with silicon-based optoelectronics^[18, 19], it has potential applications as an optical coating material^[20] and as luminescent layers. Recently, violet/blue luminescence from the CeO_x film^[21] and CeO_2 film^[22] has been reported. Europium and Samarium doped Ceria thin films have been reported to give luminescence^[23] under excitation of UV light by charge transfer transition and subsequent energy transfer to Eu^{3+} .

The luminescent properties of undoped and rare earth doped Ceria seems to depend on the preparation method. The photoluminescence spectra of CeO_2 nano rods showing unusual light emission at 370 nm, has been reportedly assigned

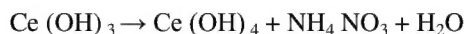
to the charge transfer transition from the localized 4f state of Cerium to the 2p valence band of Oxygen ^[24]. The charge transfer emission is independent of the morphology of the sample and so it should occur in bulk CeO₂ also. However, no emission is generally observed for bulk CeO₂. It is besides, well-known that certain oxides, like SnO₂, ZrO₂, CaO, or silica, show efficient defect luminescence ^[25, 26]. Hence the emission in CeO₂nanorods may come from the deficiency of oxygen. The reported excitation wavelength of CeO₂: Eu made using solid state reaction lies at 373 nm, while it occurs at 340 nm in CeO₂: Eu prepared by the Pechini sol-gel process ^[27, 28]. In both the cases, the nature of excitation spectrum has been attributed to charge transfer transition from O²⁻ to Ce⁴⁺ and the nature of emission spectrum to defects like oxygen vacancy and symmetry distortion. Eu³⁺ emission is affected by defect and Ce³⁺ concentration in CeO₂: Eu synthesized by Wet chemical method ^[12]. However, characteristic Eu³⁺ emission has not been observed for nanocrystals prepared by nonhydrolytic solution route ^[29].

Synthesis

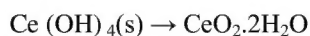
Co-precipitation reaction occurs at 50°C. The Cerous nitrate is dissolved in ethanol giving Ce³⁺ and (NO₃)⁻ ions. The reaction mechanism is given below ^[30,31].



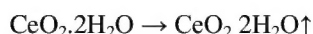
The ions undergo hydrolysis to form Ce (OH)₃. Oxidation of Ce (OH)₃ occurs readily to give yellow Ce (OH)₄ precipitates.



The formation of Ceria occurs after the oxidation of Ce³⁺ to Ce⁴⁺ in the solution at high pH (≥ 9.5). This hydroxide precipitate is transformed into an intermediate Cerium oxide dehydrate ^[31].



Calcining of this product gives Cerium oxide nanoparticles.



The heat needed for the crystals to grow is minimal. At the end of the process, metal hydroxide gel is formed which is an entangled network of polymeric chains ^[32]. The growth of crystals is arrested. The obtained Ceric hydroxide particles are washed free of anions of ammonia and nitrates and immediately kept in alcohol and thus many alcohol molecules are absorbed by the surface of the particles. Thus the growth and conservation of Ceric hydroxide nanoparticles is restrained by the protection of alcohol. Calcining the product breaks the gel to form small crystallites. The chances of agglomeration are very less and crystals with very small sizes are obtained.

Characterization

The XRD patterns were taken of Bruker D8 advance X-ray diffractometer. The 2θ range was taken from 20° to 100° in scan mode with step increment of 0.050° and step time 2 seconds at room temperature.

All the X ray reflection peaks of the XRD patterns and the respective d values could be indexed with the reported values in the JCPDS file number 4-0593 of Cerium oxide (Cerianite) precisely. This confirms the formation of CaF₂ type FCC cubic fluorite unit cell with the space group Fm3m. The value of structural parameters lattice constant a₀ and lattice volume V = a₀³ were calculated to be 0.538813 nm and 0.156428 nm³ respectively.

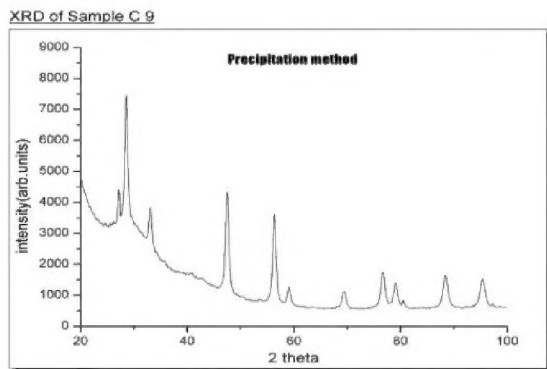


Figure 1a: X Ray Diffraction Pattern

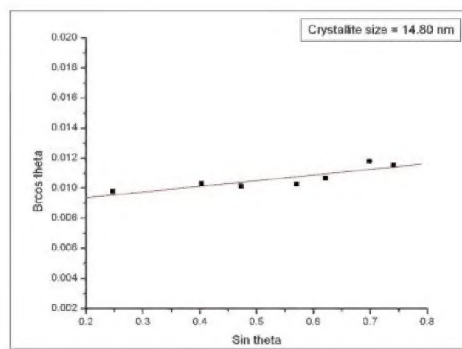


Figure 1b: Plot to Determine Crystallite Size

The average crystallite size was found to be 9.56 nm using Scherer formula and 14.8 nm by graphical method.

Fluorescence Characteristics

The fluorescence characteristics of the samples were recorded on a *Fluoromax 4* instrument of *Horiba JobinYvon* make, USA. The slit width for the excitation as well as emission monochromator was fixed at 1 nm to ensure optimization and uniformity. The integration time was kept at 0.1 second.

Figure 2a shows emission spectra of sample synthesized by Co – precipitation method. The emission characteristics were recorded for three different excitation wavelengths 345, 465 and 526 nm. There are four emission peaks observed at 590, 604, 628 and 650 nm. The intensity of the 590 nm peak relative to the other peaks is the highest among all samples. Figure 2b shows excitation spectra. The excitation spectrum was recorded by monitoring the three different emission wavelengths i.e. 590, 604, 628. There is one broad band at 345 nm and five other peaks observed at 465, 526, 532, 538 and 547 nm.

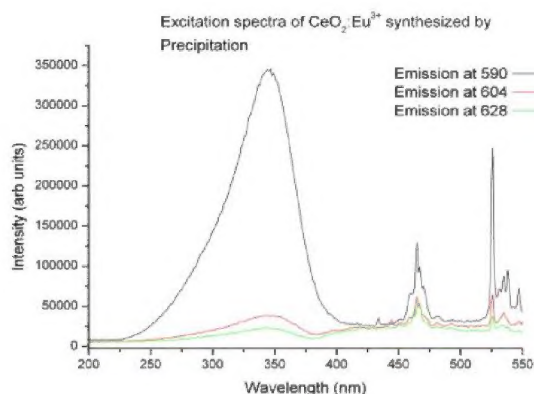


Figure 2a

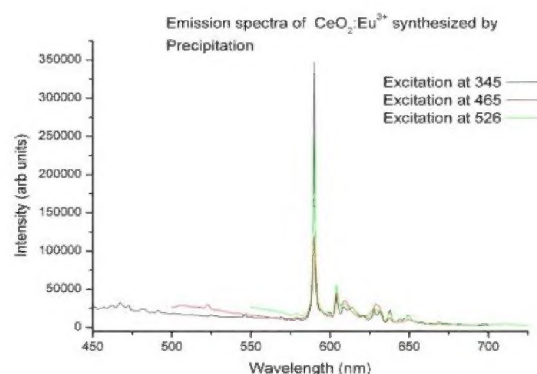


Figure 2b

The results of the fluorescence spectra confirm the incorporation of Europium in the Ceria lattice in the +3 state. The transitions of Eu^{3+} are given by $^5\text{D}_0 \rightarrow ^7\text{F}_J$ ($J = 0, 1, 2, 3, 4$) are authentically pronounced in these spectra ^[55]. The relative intensities of these transitions vary from sample to sample. The major emission peak in all the samples has been found to be at 590 nm, ascribed to the $^5\text{D}_0 \rightarrow ^7\text{F}_1$ transition, which operates by magnetic dipole interaction ^[56]. This transition is not affected by the crystal field. The other peaks at 609 nm, 632 nm ($^5\text{D}_0 \rightarrow ^7\text{F}_2$) and 654 nm ($^5\text{D}_0 \rightarrow ^7\text{F}_3$) are electric dipole transitions ^[57, 58]. These transitions are affected by the crystal field. The distribution of the excitation energy into different emission lines is shown in Figure 3.

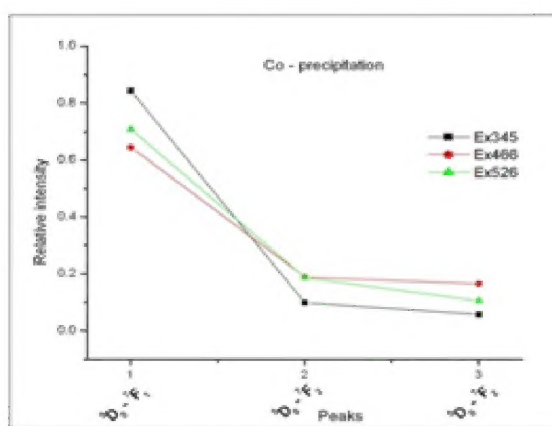


Figure 3: Distribution of Energy

The 590 nm peak is the most dominant while others are redundant. The effect of reduction in particle size is known to alter the energy levels and hence the transition probabilities. The dominance of the 590 nm peak in this case can be attributed to the reduction in the particle size.

The dominant excitation peak, which is a broad band feature can be attributed to the energy absorption by the host lattice i.e. CeO_2 [12, 33]. The multiplicity of the excitation energy levels in the host lattice leads to absorption at multiple levels, giving a broad band feature. The narrow band excitation features can be attributed to the Eu^{3+} ions. The energy absorbed by the charge transfer from O^{2-} valence band to Ce^{4+} conduction band is transferred to the Eu^{3+} and it produces red emission. The intra $4f^n$ transitions are also responsible for the excitation-emission mechanism. The $\text{Eu}-\text{O}$ bond also plays important role in the energy transfer mechanism [37]. The interactions are in terms of magnetic and electric dipole transitions [40].

Tetravalent Cerium ions (Ce^{4+}) have no $4f$ electron. This implies that CeO_2 can be a promising photoluminescence host material because of strong light absorption through the charge transfer [CT] from O^{2-} to Ce^{4+} [23]. If the energy transfer is achieved from the charge transfer state of CeO_2 to the doped rare earth ions, characteristic emissions are expected to be observed e. g. energy absorbed by the charge transfer from O^{2-} valence band to Ce^{4+} conduction band is transferred to the Eu^{3+} and produces the red emission. Rare earth doped Sr_2CeO_4 materials have already been demonstrated to exhibit excellent luminescent properties [38]. Undoped Sr_2CeO_4 gives unusual emission in blue region. The emission was assigned to a ligands-to-metal charge transfer transition of Ce^{4+} [39,40]. An efficient energy transfer can occur from the $\text{Ce}^{4+} \rightarrow \text{O}^{2-}$ charge transfer state to the trivalent RE in $\text{Sr}_2\text{CeO}_4:\text{RE}^{3+}$ (RE stands for rare earth elements) [41].

The 590 nm peak ($^5\text{D}_0 \rightarrow ^7\text{F}_1$ magnetic dipole transition) dominates the emission spectra, when the Eu^{3+} ions are located at sites with inversion symmetry. If the Eu^{3+} ions are located at sites without inversion symmetry, the 609 nm peak ($^5\text{D}_0 \rightarrow ^7\text{F}_2$ electric dipole transition) dominates [33]. Hence, increase in the 609 nm peak intensity is indicative of the increasing distortion of the local field around Eu^{3+} ions. The ratio of intensity of these two peaks i.e. ($^5\text{D}_0 \rightarrow ^7\text{F}_2 / ^5\text{D}_0 \rightarrow ^7\text{F}_1$) quantifies the degree of distortion from the inversion symmetry of the local environment of Eu^{3+} ions in the host lattice. Hence, lower the ratio, better is the inversion symmetry of Eu^{3+} ions. The dominant feature in the emission characteristics i.e 590 nm emission peak is absolutely sharp and intense while the others are practically redundant. This is significant as the width of the peak is not more than a few nano meters and the intensity is quite high. The material is likely to have a high efficiency of conversion.

REFERENCES

1. Molycorp Inc., Cerium: A Guide to its Role in Chemical Technology, USA, 1995
2. S. Tsunekawa, T. Fukuda, A. Kasuya, J. Applied Physics 87 (3) (2000) 1318
3. M. Yamashita, K. Kameyama, S. Yabe, S. Yoshida, T. Kawai, T. Sato, J. Materials Science 37 (4) (2002) 683
4. H. Abdul, Y. Iskandar, Catalysis Today 96 (3) (2004) 165
5. M. Fathi, E. Bjorgum, O.A. Rokstad, Catalysis Letters 72 (1–2) (2001) 25
6. H. Inaba, H. Tagawa, Solid State Ionics 83 (1–2) (1996) 1
7. Etsell, T. H.; Flengas, S. N. *ChemicalReview* **1970**, 70, 339
8. Subbarao, E. C.; Maiti, H. S. *Solid State Ionics* **1984**, 11, 317
9. F.H. Garzon, R. Mukundan, E.L. Brosha, Solid State Ionics 136/137 (2000) 633
10. Wang, Z. L.; Feng, X. D. *J. Physical Chemistry B* **2003**, 107, 13563
11. Miki, T.; Ogawa, T.; Haneda, M.; Kakuta, N.; Ueno, A.; Tateishi, S.; Matsuura, S.; Sato, M. *J. Physical Chemistry* **1990**, 94, 6464
12. Amit Kumar, Suresh Babu, Ajay Singh Karakoti, Alfons Schulte, and Sudipta Seal. *Langmuir* 2009 25(18), 10998 – 11007
13. Li, L.; Tao, J.; Pan, H.; Chen, H.; Wu, X.; Zhu, F.; Xu, X.; Tang, R. J. *Materials Chemistry* 2008, 18, 5363
14. N. V. Skorodumova, R. Ahuja, S. I. Simak, I. A. Abrikosov, B. Johansson, and B. I. Lundqvist *Physical Review B*, Vol 64, 115108
15. Ralph W. G. Wyckoff, *Crystal Structures*, Second Edition, Volume 1, Interscience publishers
16. Wu, J.; Wang, G. L.; Jin, D. Y.; Yuan, J. L.; Guan, Y. F.; Piper, J. *Chemical Communication* 2008, 3, 365.
17. A.M. Garrido Pedrosa, J.E.C. da Silva, P.M. Pimentel, D.M.A. Melo, F.R.G. e Silva. *J. of Alloys and Compounds* 374 (2004) 223–225
18. T. Ami, Y. Yoshida, N. Nagasawa, A. Machida, M. Suzuki, *Applied Physics Letters* 78 (2001) 1361.
19. D.Q. Shi, M. Inoescu, T.M. Silver, S.X. Dou, *Physica C* 384 (2003) 475
20. R.P. Netterfield, W.G. Sainty, P.J. Martin, S.H. Sie, *Applied Optics* 24 (1985) 2267
21. W.C. Choi, H.N. Lee, Y. Kim, H.M. Park, E.K. Kim, *Japanese J. Applied Physics* 38 (Part 1) (1999) 6392
22. G. Fei, L.I. Guo-hua, Z. Jian-Hui, Q. Fu-Guang, et al., *Chinese Physical Letters*. 18 (2001) 443
23. Shinobu Fujihara and Masashi Oikawa. *J. Applied Physics*, Vol. 95, No. 12, 15 June 2004
24. Sun, C.; Li, H.; Zhang, H.; Wang, Z.; Chen, L. *Nanotechnology* **2005**, 16, 1454
25. Green, W. H.; Le, K. P.; Grey, J.; Au, T. T.; Sailor, M. J. *Science* **1997**, 276, 1826

26. J. A.; Garcia, A.; Remo; Piqueras, J. *Physica. Status Solidi A* **1985**, 89, 237
27. Liu, X.; Chen, S.; Wang, X. *J. Luminescence*. **2007**, 127, 650
28. Guo, H.; Qiao, Y. *Appl. Surface Science* **2008**, 254, 1961
29. Zhenling Wang, ZeweiQuan, and Jun Lin. *Inorganic Chemistry*, Vol. 46, No. 13, 2007
30. S.T. Aruna and K.C. Patil, *Nano Structured Materials* Vol. 10. No. 6. 1998, 955-964.
31. R.D. Purohita, B.P. Sharma, K.T. Pillai, A.K. Tyagi, *Materials Research Bulletin* 36 (15) 2001, 2711
32. E. Nachbaur, E. Baumgartner and J. Schober, *Proceedings of the 2nd European Symposium on Thermal Analysis* (1981), 417.
33. M. Wynne, *J. Chem. Educ.* 64 (1987) 180
34. J. J. KINGSLEY and K.C. PATIL, *Materials letters*, 6,198, 427-432
35. G. K. Adams, W.G. Parker and H.G. Wolfhard, *Discussions Faraday Society* 14, 1953, 97.
36. A K Tyagi, *International Symposium on Advanced Materials and Processing*, 6-8 December 2004, I. I. T, kharagpur, India
37. Lina Gu, GuangyaoMeng, *Materials Research Bulletin*, 2007
38. E. Danielson, M. Devenney, D. M. Giaquinta, J. H. Golden, R. C. Haushalter, E. W. McFarland, D. M. Poojary, C. M. Reaves, W. H. Weinberg, and X. D. Wu, *Science* **279**, 837 1998
39. Lee, Y. E.; Norton, D. P.; Budai, J. D.; Rack, P. D.; Potter, M. D. *Applied Physics Letters* **2000**, 77, 678.
40. Goubin, F.; Rocquefelte, X.; Whangbo, M. H.; Montardi, Y.; Brec, R.; Jobic, S. *Chemistry Materials* **2004**, 16, 662
41. Hirai, T.; Kawamura, Y. *J. Physical Chemistry B* **2004**, 108, 12763